Fluorescence lifetime imaging in turbid media

M. A. O'Leary, D. A. Boas, X. D. Li, B. Chance, and A. G. Yodh

Department of Physics and Astronomy and Department of Biochemistry and Biophysics, University of Pennsylvania, Philadelphia, Pennsylvania 19104

Received August 15, 1995

The lifetime of a fluorophore generally varies in different environments, making the molecule a sensitive indicator of tissue oxygenation, pH, and glucose. However, lifetime measurements are complicated when the fluorophore is embedded in an optically thick, highly scattering medium such as human tissue. We formulate the inverse problem for fluorescence lifetime tomography using diffuse photon density waves, and we demonstrate the technique by deriving spatial images of heterogeneous fluorophore distribution and lifetime, using simulated measurements in heterogeneous turbid media. © 1996 Optical Society of America

The lifetime and number density of fluorophores in human tissue can potentially provide information about tissue oxygenation, pH, and glucose.[1] Tissue fluorescence measurements are generally made by use of fluorophores at or near the surface[2]; only recently have investigators begun to develop the methods needed to extract the fluorophore lifetime information from deep within heterogeneous turbid media.[3–7] Diffuse fluorescence in deep tissues has been explored primarily as a means of tumor detection by locating the center of fluorescing objects.[8–10] This approach relies on the fact that the fluorophore will preferentially accumulate in tumors.[11] In this Letter we demonstrate a method whereby one can simultaneously derive a spatial map of the concentration and lifetime of heterogeneous fluorophore distributions, using variations in the amplitude and phase of fluorescent diffuse photon density waves (DPDW's).

The propagation of photons through a highly scattering medium with low absorption is well described by the diffusion equation.[12] In this case an amplitude-modulated point source of photons introduced into a diffusive medium produces a DPDW.[13–15] The wave number k of the DPDW is a function of the medium absorption coefficient μ_a, reduced scattering coefficient μ_s', and the source modulation frequency f. μ_a and μ_s' depend on optical wavelength. In a homogeneous infinite medium the spatial part of the DPDW at a position $\mathbf{r}$ generated by a point source of amplitude A (in units of photons per second) located at the origin is $U_0(\mathbf{r}, k) = A \exp(ikr)/4\pi Dr$ and $k^2 = (-v\mu_a + i\omega)/D$. Here $D = v/(3\mu_s')$ is the photon diffusion coefficient and v is the speed of light in the medium. $\omega = 2\pi f$ is the angular modulation frequency of the source. If a localized fluorophore with volume d^3r and with lifetime τ is embedded within this medium at a position $\mathbf{r}$, the fluorescent photon density δu_{fl} measured at a detector position $\mathbf{r}_d$ for a source at $\mathbf{r}_s$ is[16]

$$\delta u_{\mathrm{fl}}(\mathbf{r}, \mathbf{r}_s, \mathbf{r}_d) = U_0(\mathbf{r}_s - \mathbf{r}, k^{\lambda 1}) \frac{\eta(\mathbf{r})}{1 - i\omega\tau(\mathbf{r})} \frac{v}{D^{\lambda 2}} \times G(\mathbf{r}_d - \mathbf{r}, k^{\lambda 2}) d^3 r . \quad (1)$$

Here the wave number $k^{\lambda 1}$ ($k^{\lambda 2}$) depends on the optical properties of the medium at the excitation (fluorescent) wavelength $\lambda 1$ ($\lambda 2$). Equation (1) has three pieces: $U_0(\mathbf{r}, k^{\lambda 1})$ represents the demodulation and phase shift that are due to the excitation wave's passage from the source (at $\mathbf{r}_s$) to the fluorophore at $\mathbf{r}$, $\eta(\mathbf{r})/[1 - i\omega\tau(\mathbf{r})]$ represents the demodulation and phase shift that are due to the strength and lifetime of the fluorphore, and $vG(\mathbf{r}_d - \mathbf{r}, k^{\lambda 2})/D^{\lambda 2} = v \exp(ik^{\lambda 2}|\mathbf{r}_d - \mathbf{r}|)/4\pi D^{\lambda 2}|\mathbf{r}_d - \mathbf{r}|$ represents the demodulation and phase shift that are due to passage of the reradiated wave from $\mathbf{r}$ to the detector at $\mathbf{r}_d$. η is the product of the fluorophore absorption coefficient and fluorescence quantum yield. For a weakly absorbing spatial distribution of fluorophores, the fluorescent photon density wave may be determined by integration over the contributions from all fluorophores:

$$U_{\mathrm{fl}}(\mathbf{r}_s, \mathbf{r}_d) = \int d^3 r \delta u_{\mathrm{fl}}(\mathbf{r}, \mathbf{r}_s, \mathbf{r}_d) . \quad (2)$$

Hereafter we refer to U_{fl} as the fluorescent DPDW. This model is an approximation because U_0 and G neglect the effects of heterogeneities on photon propagation from source to fluorophore and from fluorophore to detector. In principle, U_0 and G may be updated to include the effects of heterogeneities. The model also assumes that there are no saturation or photon quenching effects.

The fluorescence model in Eq. (2) is of the same form as the first-order perturbation model for a scattering medium with inhomogeneous absorption.[17] Thus it should be feasible to generate images for $\eta(\mathbf{r})$ and $\tau(\mathbf{r})$ by using standard imaging algorithms. (The reconstruction differs from the pure absorption case in that the reconstructed quantity is now complex and is a function of the modulation frequency.) In these reconstruction algorithms we digitize the integral in Eq. (2), $[\eta(\mathbf{r}), \tau(\mathbf{r}), \mathbf{r} \Rightarrow \eta_j, \tau_j, r_j]$, and for a series of measurements made at source–detector positions $\mathbf{r}_{si}$, $\mathbf{r}_{di}$ generate the following matrix equation:

$$U_{\mathrm{fl}}(\mathbf{r}_{si}, \mathbf{r}_{di})_i = \sum_{j=1}^{N_{\mathrm{voxels}}} \delta u_{\mathrm{fl}}(\mathbf{r}_j, \mathbf{r}_{si}, \mathbf{r}_{di}) d^3 r_j . \quad (3)$$

This matrix equation can be inverted or solved by many techniques. We have used an algebraic reconstruction method to solve for the real and imaginary parts of the unknown, $\eta_j/(1 - i\omega\tau_j)$.[18] (The ratio of the imaginary and real parts of the solution yields τ, and then η is calculated.)

0146-9592/94/020158-03$6.00/0

In this study computer-generated data are obtained from exact solutions to Eq. (4) for the case of a fluorescent sphere in a uniform background.[19] Using forward amplitude and phase data (with added 1% amplitude and 0.1° phase noise), we have reconstructed images of η and τ. The measurement geometry is described in Fig. 1(a). In the first set of reconstructions all fluorophores are located in the object, and there is no background fluorescence. In Figs. 1(b) and 1(d) we demonstrate a reconstruction proportional to the fluorophore concentration with source modulation frequencies of 50 and 150 MHz, respectively.

While implementing these reconstructions we found that some isolated voxels had unphysically high values for both η and τ. These voxels do not contribute significantly to the total signal since the quantity $\eta/\omega\tau$ is comparable with or smaller than that of the neighboring voxels. As part of our image analysis, we identified these voxels and replaced η and τ with the nearest-neighbor averages. We determined the object size by including any voxel with a fluorophore concentration of at least 50% of the maximum fluorophore concentration. The lifetime reported was the average lifetime of these voxels. Figures 1(c) and 1(e) (open squares) exhibit good agreement between the average reconstructed value of the lifetime and its known value. Generally we found that the lifetime reconstructions are more accurate at low source modulation frequencies, for which the occurrence of these spurious voxels is less frequent and the intrinsic phase shift that is due to the lifetime of the fluorophore [$\phi = \tan^{-1}(\omega\tau)$] is far from its saturation value ($\pi/2$).

The image quality is improved if some *a priori* information is given. For example, if the fluorphore distribution is known, then lifetime-only reconstructions are possible and are shown in Figs. 1(c) and 1(e) (filled circles).

In typical clinical situations there will also be a fluorophore outside the region. In this case we separate the contributions from inside and outside the heterogeneous region:

$$U_{\mathrm{fl}}(\mathbf{r}_s, \mathbf{r}_d) = \int_{\text{all space}} d^3r U_0(\mathbf{r} - \mathbf{r}_s, k^{\lambda 1}) \times \frac{\eta_0}{1 - i\omega\tau_0} \frac{v}{D^{\lambda 2}} G(\mathbf{r}_d - \mathbf{r}, k^{\lambda 2}) + \int_{\text{heterogeneity}} d^3r \times U_0(\mathbf{r} - \mathbf{r}_s, k^{\lambda 1}) \left[\frac{\eta(\mathbf{r})}{1 - i\omega\tau(\mathbf{r})} - \frac{\eta_0}{1 - i\omega\tau_0} \right] \times \frac{v}{D^{\lambda 2}} G(\mathbf{r}_d - \mathbf{r}, k^{\lambda 2}). \quad (4)$$

Here η_0 and τ_0 are the fluorescence properties outside the heterogeneity and η and τ are the florescence properties inside the heterogeneity. Hereafter we will refer to the first term on the right-hand side of Eq. (4) as U_{bg}. If the object contrast is high, i.e., $\eta(\mathbf{r})/[1 - i\omega\tau(\mathbf{r})] \gg \eta_0/(1 - i\omega\tau_0)$, then the fluorescent signal that is due to the heterogeneity, $\Delta U_{\mathrm{fl}} = U_{\mathrm{fl}} - U_{\mathrm{bg}}$, is given by

$$\Delta U_{\mathrm{fl}}(\mathbf{r}_s, \mathbf{r}_d) = \int d^3r U_0(\mathbf{r} - \mathbf{r}_s, k^{\lambda 1}) \times \frac{v\eta(\mathbf{r})}{1 - i\omega\tau(\mathbf{r})} \frac{v}{D^{\lambda 2}} G(\mathbf{r}_d - \mathbf{r}, k^{\lambda 2}). \quad (5)$$

To accomplish this subtraction, one may use analytic solutions for U_{bg}.[19] However, this method requires knowledge of the background lifetime and concentration, which may not be possible in clinical situations. Another option is to eliminate the background signal by subtraction of two measurements having the same source–detector separation, as shown in Fig. 2(a). In these difference measurements the background (homogeneous) fluorescent contribution will cancel, and only

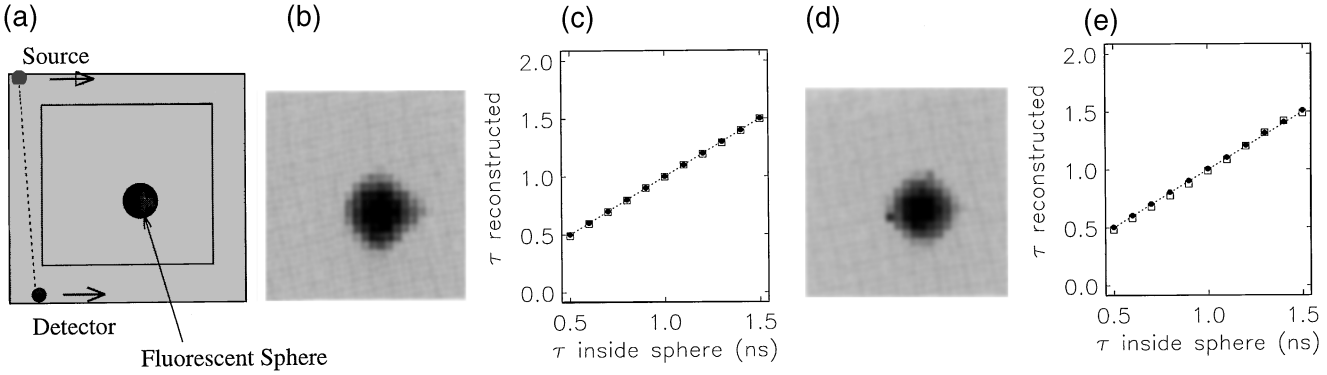

Fig. 1. (a) Scanning geometry consists of a source and a detector scanning every 0.2 cm about the four sides of a 7.0 cm × 7.0 cm square in an infinite medium. The reconstruction area is a slab of area 5.0 cm × 5.0 cm and height 1.0 cm. The optical properties of the media are $\mu_s' = 10\ \mathrm{cm}^{-1}$ everywhere, μ_a (chromophore) $= 0.03\ \mathrm{cm}^{-1}$ everywhere for both the excitation and the emission wavelength, and μ_a (fluorophore, inside the sphere) $= 0.02\ \mathrm{cm}^{-1}$ at the excitation wavelength and $0.01\ \mathrm{cm}^{-1}$ at the emission wavelength. The source modulation frequency is 50 MHz. (b) Reconstruction of the fluorophore concentration for the system described in (a). The lifetime inside the 1.0-cm-diameter sphere is 0.6 ns. The gray scale ranges from 0 cm^{-1} (white) to 0.007 cm^{-1} (black). 2500 SIRT iterations were performed with a constraint on both concentration ($0.0 \le \eta \le 0.1\ \mathrm{cm}^{-1}$) and lifetime ($0 \le \tau \le 10$ ns). (c) Using this setup, we varied the actual lifetime of the fluorophore from 0.5 to 1.5 ns, and the average reconstructed lifetime was calculated. The open squares are derived from a reconstruction of both fluorophore concentration and lifetime, and the filled circles are derived from the lifetime reconstruction only. (d), (e) Same as (b), (c), except that the source modulation frequency has been increased to $f = 150$ MHz. The gray scale in (d) ranges from 0 cm^{-1} (white) to 0.009 cm^{-1} (black).

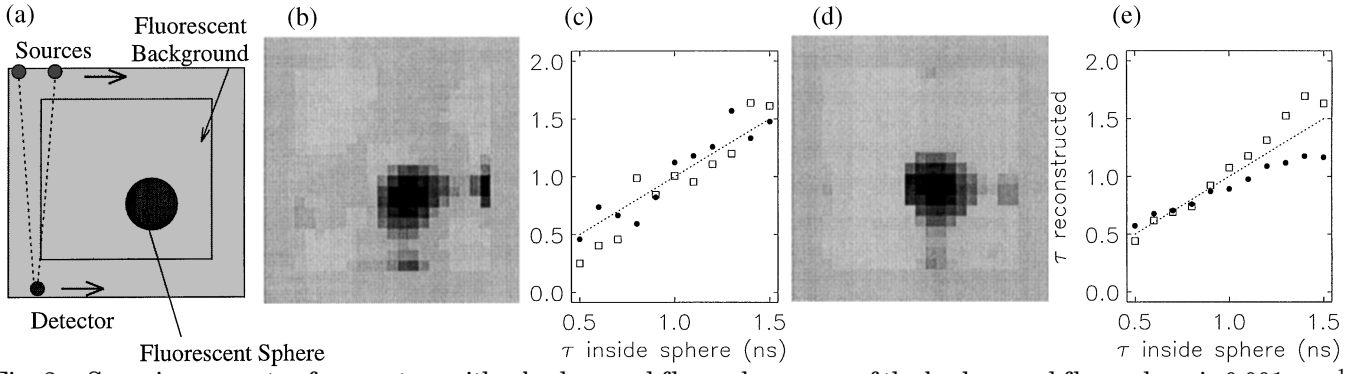

Fig. 2. Scanning geometry for a system with a background fluorophore. μ_a of the background fluorophore is 0.001 cm^{-1} at the excitation wavelength and 0.005 cm^{-1} at the emission wavelength, and the lifetime is 1.0 ns. The setup is the same as in Fig. 1(a) with the addition of the background fluorophore and a second source 0.6 cm from the first. (b) Reconstruction of the heterogeneous fluorophore distribution for the system described in (a). The lifetime inside the 1.5-cm-diameter sphere is 0.6 ns. The gray scale ranges from 0 cm^{-1} (white) to 0.017 cm^{-1} (black). 2500 SIRT iterations were performed with a constraint on both concentration ($0.0 \leq \eta \leq 0.1\ cm^{-1}$) and lifetime ($0 \leq \tau \leq 10$ ns). (c) Average reconstructed lifetime for a series of reconstructions, with the setup in (a). The open squares are derived from a reconstruction of both fluorophore concentration and lifetime. The filled circles are derived from the lifetime reconstruction only. (d), (e) Same as (b), (c), except that the source modulation frequency has been increased to $f = 150$ MHz. The gray scale in (d) ranges from 0 cm^{-1} (white) to 0.020 cm^{-1} (black).

the inhomogeneous part will remain. This method has been employed successfully in absorption reconstructions to reduce the importance of accurate knowledge of the background optical properties.[17] Note that in these images the fluorescent properties of the heterogeneities have been reconstructed; no information about the background fluorescence is derived.

Figure 2(a) depicts the scanning geometry used for a system with fluorophore both inside and outside the sphere (radius 0.75 cm). Images of concentration are shown in Figs. 2(b) and 2(d) for source modulation frequencies of 50 and 150 MHz, respectively. The average reconstructed lifetime calculated over the area of the sphere is plotted in Figs. 2(c) and 2(e) for a series of reconstructions on objects with different lifetimes inside the sphere.

We have demonstrated an algorithm by which the heterogeneous fluorophore distribution and lifetime in a turbid medium may be obtained from tomographic measurements of diffusing photon distributions. The solution for finite systems may be obtained by application of the appropriate boundary conditions.

We thank Eva Sevick-Muraca for useful discussions that emphasized to us the importance of the fluorescence lifetime measurements. A. G. Yodh acknowledges support from National Science Foundation grants DMR-93068114 and DMR-9058498 and the Alfred P. Sloan Foundation. B. Chance acknowledges support in part by National Institutes of Health grants NS-27346, HL-44125, and CA-50766/60182.

References

1. S. B. Bambot, J. R. Lakowitz, and G. Rao, Trends Biotechnol. **13,** 106 (1993).
2. D. W. Piston, M. S. Kirby, H. P. Cheng, W. J. Lederer, and W. W. Webb, Appl. Opt. **33,** 662 (1994).
3. E. M. Sevick-Muraca and C. L. Burch, Opt. Lett. **19,** 1928 (1994). See also C. L. Hutchinson, T. L. Troy, and E. M. Sevick-Muraca, Proc. Soc. Photo-Opt. Instrum. Eng. **2389,** 274 (1995).
4. M. S. Patterson and B. W. Pogue, Appl. Opt. **33,** 1963 (1994).
5. B. J. Tromberg, S. Madsen, C. Chapman, L. O. Svaasand, and R. C. Haskell, in *Advances in Optical Imaging and Photon Migration,* R. R. Alfano, ed., Vol. 21 of OSA Proceedings Series (Optical Society of America, Washington, D.C., 1994), p. 93.
6. A. J. Durkin, S. Jaikumar, N. Ramanujam, and R. Richards-Kortum, Appl. Opt. **33,** 414 (1994).
7. J. Wu, M. S. Feld, and R. P. Rave, Appl. Opt. **32,** 3585 (1993).
8. A. Knuttel, J. M. Schmitt, R. Barnes, and J. R. Knutson, Rev. Sci. Instrum. **64,** 638 (1993).
9. M. A. O'Leary, D. A. Boas, B. Chance, and A. G. Yodh, J. Lumin. **60–61,** 281 (1994); D. A. Boas, M. A. O'Leary, B. Chance, and A. G. Yodh, Phys. Rev. E **47,** R2999 (1993).
10. J. Wu, Y. Wang, L. Perelman, I. Itzkan, R. R. Desari, and M. S. Feld, Opt. Lett. **20,** 489 (1995).
11. X. D. Li, B. Beauvoit, R. White, S. Nioka, B. Chance, and A. G. Yodh, Proc. Soc. Photo-Opt. Instrum. Eng. **2389,** 789 (1995).
12. M. S. Patterson, B. Chance, and B. C. Wilson, Appl. Opt. **28,** 2331 (1989).
13. J. B. Fishkin and E. Gratton, J. Opt. Soc. Am. A **10,** 127 (1993).
14. A. G. Yodh and B. Chance, Phys. Today **48**(3), 34 (1995).
15. M. A. O'Leary, D. A. Boas, B. Chance, and A. G. Yodh, Phys. Rev. Lett. **69,** 2658 (1992).
16. Eq. (2) is the Fourier transform of the time-domain equation presented by Sevick-Muraca *et al.*[3] and was presented in a similar form by Patterson and Pogue.[4]
17. M. A. O'Leary, D. A. Boas, B. Chance, and A. G. Yodh, Opt. Lett. **20,** 426 (1995).
18. A. C. Kak and M. Slaney, *Principles of Computerized Tomographic Imaging* (Institute of Electrical and Electronics Engineers, New York, 1988), Chap. 6, p. 211.
19. X. D. Li, M. A. O'Leary, D. A. Boas, B. Chance, and A. G. Yodh, "Fluorescent diffuse photon density waves in homogeneous and heterogeneous turbid media: analytic solutions and applications," Appl. Opt. (to be published).